Volume 11
Number 10
14 March 2020
Pages 2575–2864

Chemical Science

rsc.li/chemical-science

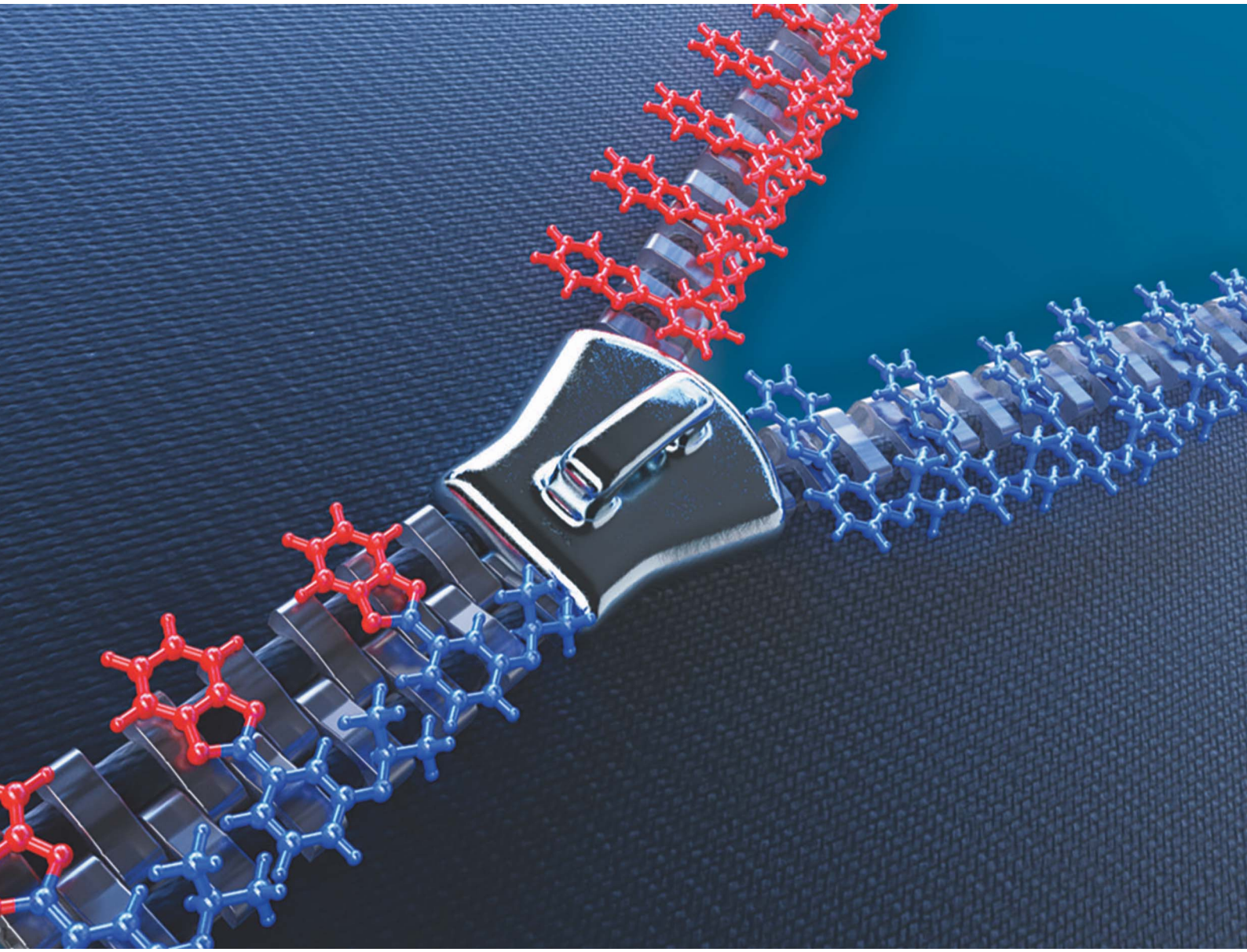

ISSN 2041-6539

ROYAL SOCIETY OF CHEMISTRY

EDGE ARTICLE
Panče Naumov *et al.*
Efficiently self-healing boronic ester crystals

Chemical Science

ROYAL SOCIETY OF CHEMISTRY

EDGE ARTICLE

View Article Online
View Journal | View Issue

Cite this: *Chem. Sci.*, 2020, **11**, 2606

All publication charges for this article have been paid for by the Royal Society of Chemistry

Received 7th November 2019
Accepted 25th January 2020

DOI: 10.1039/c9sc05640h

rsc.li/chemical-science

Efficiently self-healing boronic ester crystals†

Patrick Commins, [a] Marieh B. Al-Handawi, [a] Durga Prasad Karothu, [a] Gijo Raj [a] and Panče Naumov *[ab]

The perception of organic crystals being rigid static entities is quickly eroding, and molecular crystals are now matching a number of properties previously thought to be unique to soft materials. Here, we present crystals of a boronate ester that encompass many of the elastic and plastic mechanical properties of polymers such as bending, twisting, coiling and highly efficient self-healing of up to 67%, while they maintain their long-range structural order. The approach utilizes the concept of dynamic covalent chemistry and proves it can be applied towards ordered materials. This work expands our current understanding of the properties of crystalline molecular materials, and it could have implications towards the development of mechanically robust organic crystals that are capable of self-repair for durable all-organic electronics and soft robotics.

Introduction

Fatigue and wear are some of the most inevitable, yet undesirable fates of a material. A deviation from this common axiom was introduced by self-healing materials that are capable of autonomously recovering from damage.[1] The self-healing effect has been extensively explored in mesophasic materials and many self-healing polymers have been developed that use encapsulation,[2,3] metal–ligand interactions,[4,5] hydrogen bonding,[6,7] dynamic covalent chemistry,[8] pericyclic reactions,[9,10] and other covalent and supramolecular strategies.[11–14] Being inherently less flexible, the deformation of molecular crystalline solids has been given much less attention, however this view is evolving to appreciate the vibrant properties of crystalline solids.[15–19] More recently, the realm of atypical phenomena found in crystalline solids has been expanded by the discovery of methods to 'weld' crystals[20] and the first self-healing organic crystal,[21] although the material in the latter case showed a modest recovery of only less than 7%. We hypothesized that self-healing in molecular crystals is a more general property and it may be found by exploring other dynamic covalent chemistry motifs.[22,23] To that end, we focused on the reversible reactions between boronic acids and boronic esters that have been utilized to create self-healing polymers and hydrogels.[24–26] Here, we report crystals of a boronic ester that are capable of self-healing with an initial healing of 67% to 44% after five cycles. This material is unique in that unlike other organic crystals that can bend either elastically or plastically,[27,28] when exposed to local pressure it can be deformed elastically and plastically by bending, twisting and coiling while maintaining most of its crystallinity. By providing the first example of highly efficient repair of an organic crystal, this material bridges the gap between soft matter and ordered crystalline solids, and opens prospects for the discovery of other self-healing crystalline materials.

Results

While screening various boronic acids, the 3-isopropoxyphenyl boronic acid (**1**) was selected and its catechol ester (**3**) was synthesized (Fig. 1A).[29] The product was recrystallized from *n*-hexane to yield translucent planks of up to 3 cm in length. The crystals can be bent plastically, twisted elastically, and shaped into arbitrary morphologies, as demonstrated by using crystals to write in English and Arabic (Fig. 1B). When the crystals are pressed on their (100) face they bend and remain bent indefinitely, but can be flattened by applying force in the opposite direction or by uniform pressing across the kink (Movies S1 and S2†). The bending and flattening can be repeated at least five times, and the crystals retain their macroscopic integrity. Unlike bending, however, when the crystals are twisted around their long axis ([010]), they return to their original shape after the torque has been removed (Movie S3†).

As confirmed with XRD, the crystals before bending are single crystals (Fig. S1†), but they are notably soft. The elastic modulus on the (100) face, measured using three-point bending tests, was determined to be 4.8–27.2 MPa (Fig. S2 and Table S1†) and thus are about tenfold lower than low-density polyethylene (94.8 ± 3.1 MPa).[30] To test the limits of their extraordinary elasticity, an elongated crystal was twisted by using a torque-

[a]*New York University Abu Dhabi, Abu Dhabi, POB 129188, United Arab Emirates. E-mail: pance.naumov@nyu.edu*

[b]*Radcliffe Institute for Advanced Study, Harvard University, 10 Garden St., Cambridge, MA 02138, USA*

† Electronic supplementary information (ESI) available. CCDC 1828493. For ESI and crystallographic data in CIF or other electronic format see DOI: 10.1039/c9sc05640h

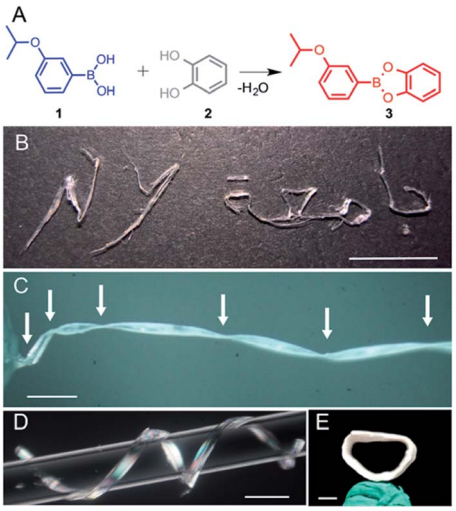

Fig. 1 Preparation and mechanical reconfiguration of crystals of 3-isopropoxyphenylboronic acid catechol ester, **3**. (A) A general scheme for preparation of the ester (**3**) from 3-isopropoxyphenyl boronic acid (**1**) and catechol (**2**). (B) Several crystals of **3** shaped to write 'N. Y. Jameia' ('N. Y. University' in Arabic). (C–E) Crystals of **3** that have been twisted 1080° (C), coiled around a glass capillary (D), and that have had their two ends mended together to form a crystal ring (E). Scale bars: (B) 1 cm; (C) 1 mm; (D) 2 mm; (E) 1 mm.

transducing device over 1080° (three full revolutions) before it snapped from one end (Fig. 1C and Movie S4†). Upon breaking, the crystal spontaneously partially untwisted, and only two out of the four kinks were retained. Crystals can also be manually coiled around a glass capillary and shaped into a helix with arbitrary pitch and diameter (Fig. 1D and Movie S5†). The coiling is plastic, and the original shape of the crystal can only be recovered by manual flattening. The crystal can be coiled and uncoiled repeatedly, however rippling and delamination occur on the surface. Surprisingly, we found that a coiled crystal can even be mended in 24 hours by compressing the two ends together (Fig. 1E and Movie S6†), indicating that it can repair itself, analogous to the self-healing of polymers and elastomers.[1–14]

The SEM images of deformed or broken crystals (Fig. S3†) hint at plausible mechanism of the different modes of crystal deformation (bending, twisting and coiling). Upon bending, the shear stress between the sheets is released by delamination into major slabs (thickness, 37 ± 6 μm) and minor sheets (5.8 ± 1.1 μm) that appear as striations normal to the bent face, and this accounts for the plastic behavior of the crystals (Fig. S3A and B†). During moderate twisting the striations were not observed; hence, the crystal does not delaminate, and it unwinds to recover its original shape after the torque was removed (Fig. S3C and D†). Coiling in a helix is a combination of bending (plastic deformation) and twisting (elastic deformation),[15] and the crystal remains coiled due to the dominant contribution of the plastic component to the overall deformation (Fig. S3E†). Upon uncoiling the layers on the convex surface delaminate and buckle, similar to what was observed upon straightening of a bent crystal (Fig. S3F†). In stark contrast with the flexible mechanical reconfigurations described above, applying force to the $(10\bar{2})$ face results in fracture (Fig. S3G and H, and Movie S7†).

The mechanical response can be scrutinized by the anisotropy in crystal packing and absence of strong intermolecular interactions (Fig. 2). In the crystal structure of **3** the molecules pack in head-to-head arrangement to form alternating infinite chains interacting through π–π interactions, with closest distances between ring centroids of 3.545(1) and 3.628(1) Å, which ultimately form sheets of molecules. We hypothesize that when pressure is applied on the (100) face, the van der Waals interactions between sheets allow the molecules to glide over each other and the dislocations to move unobstructed to achieve bending (Movie S8†). This process is conceptually similar to planes of sliding clay commonly found in geology.[31] Additionally, the π–π interactions in between molecules provide structural flexibility so that they can be compressed or spaced further apart. As shown by the strong and discrete X-ray diffraction peaks in Fig. 3A–D, the crystals retain a high degree of crystallinity throughout the mechanical deformation after being bent and unbent up to 20 times. We note that after repeated bending (>5–10 cycles) the diffraction spots become less discrete and the sample appears more polycrystalline. In line with the expected accumulation of defects, the mosaicity of an unbent crystal changed from 0.58° to 1.73° when it was bent and unbent 20 times. The preservation of crystal integrity indicates that such plastically bendable crystals display a restorative mechanism at the interface between the sliding slabs that partially repairs their crystalline lattice, thus preventing disintegration.

In elastic deformation, such as moderate twisting, the crystal deforms in response to strain that can be approximated by two forces acting in opposite directions along the long axis of the crystal.[15] The lattice of the entire crystal is deformed within the elastic deformation regime, and no significant delamination occurs. After the forces are removed, the expanded portions of the crystal shrink and the crystal restores its original shape.[27] On the contrary, the mechanism of plastic bending implies that irreversibly bendable crystals inevitably bend by motion of dislocations which eventually results in delamination into layers.[32] The intermolecular interactions between the surface molecules of the intimately contacted layers after sliding must be restored to prevent the bent crystal from recovering its original shape. The ability of molecules to slide past each other along slip-planes provides a degree of flexibility in their orientation, which could allow healing at the interface by swapping of partner molecules, whereby the contact across the gliding interface is preserved. When pressure is applied to the $(10\bar{2})$ face of the crystal, the crystal simply breaks (Movie S9†). We propose that this happens because the force is in plane with the π–π interactions and the slip planes cannot dissipate the stress. The alignment into π-stacked infinite chains provides an additional degree of flexibility that allows the crystals to twist. Unlike bending, however the twisting applies a torsional strain in the [010] direction, and thus in the direction of the π–π interactions (Movie S10†). A twist along this axis strains the π–π interactions as the stacked molecules rotate away from an optimal geometry. When the torque is removed, the structure responds by restoring the ideal configuration to maximize the π–π overlap

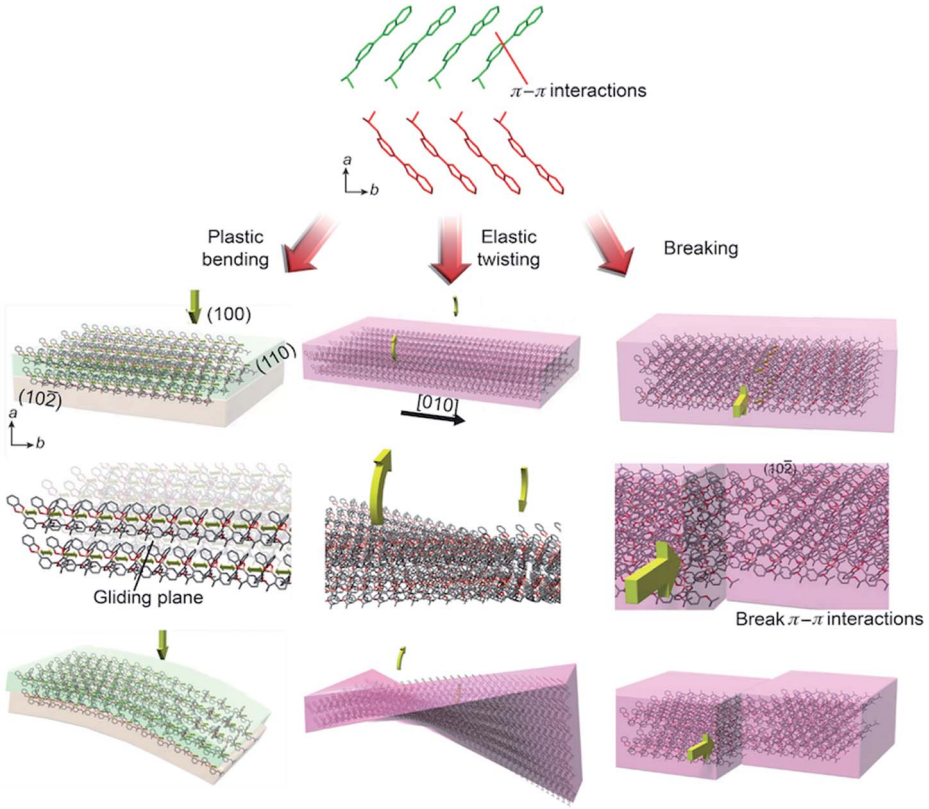

Fig. 2 Crystal structure of **3** and mechanism of plastic bending, elastic twisting and breaking of its single crystals. During bending the layers of molecules slide past each other along glide planes bound by π–π interactions (the closest centroid-to-centroid distances are 3.545(1) and 3.628(1) Å). The twisting rotates molecules around the [001] direction which strains, but does not break the π–π interactions. When force is applied in plane of the π–π interactions, the crystal breaks.

and this allows the material to respond elastically. van der Waals interactions could also contribute to the plastic and elastic behavior.

To test the self-healing ability, the crystal was adhered to the silicone pads of a small tensile tester and bifurcated while measuring the stress required to induce the virgin break by pulling the sample in the [100] direction of the crystal (Fig. S4A†). The Young's modulus of the (10$\bar{2}$) face of the crystal was determined to be 1.18 MPa from the stress–strain profile (Fig S4B†). This value is low compared to the other organic crystals (on the order of 0.1–10 GPa), and indicates the pronounced softness of the material. The two pieces of the separated crystal were then brought in contact across the new interface using a minimal pressure (~1 MPa) that was required to keep them in contact with each other, and left to heal. After 24 hours, the sample was separated and the change in force was monitored during the separation (Fig. 4A).

At low displacement (<0.12 mm), the load rapidly increases due to decompression of the silicone pads. At larger displacements the crystal begins to experience a tensile load and the load incrementally grows until a breaking point occurs at 0.063 N (49.6 kPa), and the fragments separate. Typically, a breakpoint in a material is represented by a sudden drop in the load (Fig. S4B†). However, these crystals were found to peel away from each other during tensile stress, which manifested as a much more gradual drop in the load, as shown in Fig. 4A at displacements from 0.32–0.39 mm and it is this drop in the load that is representative of the adhesion between the two surfaces as it is the amount of force holding the pieces together. If there was no adhesion between the two pieces they would simply be pulled apart and there would be no force registered (Fig. S5†). Relative to the strength of the virgin crystal (74.0 kPa), the difference between the highest load before and after the break normalized by the surface area of the healed interface gives a healing of 67%. Compared to the previously reported example of self-healing in dipyrazolethiuram disulfide crystals (~7%),[21] this represents an order of magnitude improvement in the healing efficiency. This result is the highest reported self-healing ability of molecular crystals, and it is comparable with soft self-healing materials such as polymers.

Subsequent healing attempts were repeated five times in succession on the same crystal, and showed a recovery of 58, 62, 47 and 44% from the second to the fifth healing cycle. Such decrease in recovery over repeated attempts is common for self-healing polymeric materials,[33] and we attribute the fatigue to accumulation of defect sites or areas of lost contact over repeated separations. Additional reasons for the decreased self-healing efficiency over repeated attempts may be separation of debris and the difficulty to accomplish good alignment of the fragments due to small shifts. However, the crystallinity in the

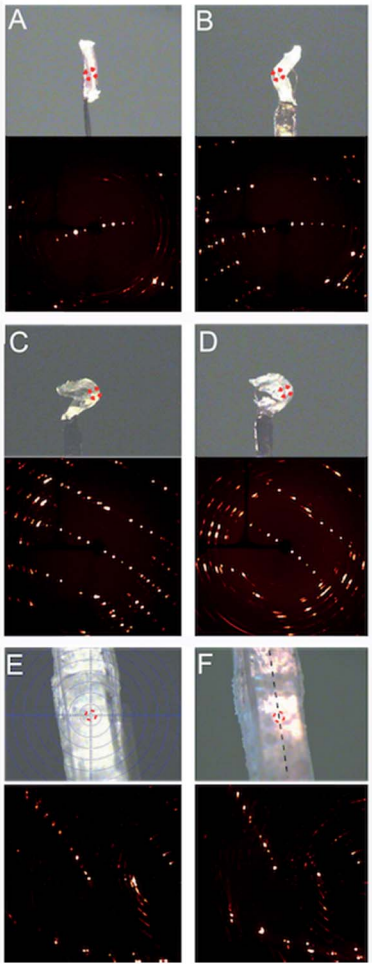

Fig. 3 X-ray diffraction pattern of a plastically bent crystal of **3** before and after bending and healing. (A) An unbent crystal (crystal mosaicity, 0.58°), (B) a bent crystal, (C) the same crystal bent 10 times and (D) the same crystal bent 20 times (crystal mosaicity, 1.73°). X-ray diffraction patterns obtained with a narrow X-ray beam (20–40 μm) for the same crystal before healing (E) and after healing (F). The Bragg peaks from the healed crystal do not show significant change after being kept in contact for 24 h, and thus it is inferred that the crystallinity of the bulk of the material was preserved during the healing. The diffraction was obtained by restricting the ω, κ and φ angles. The corresponding diffraction patterns are below the optical images.

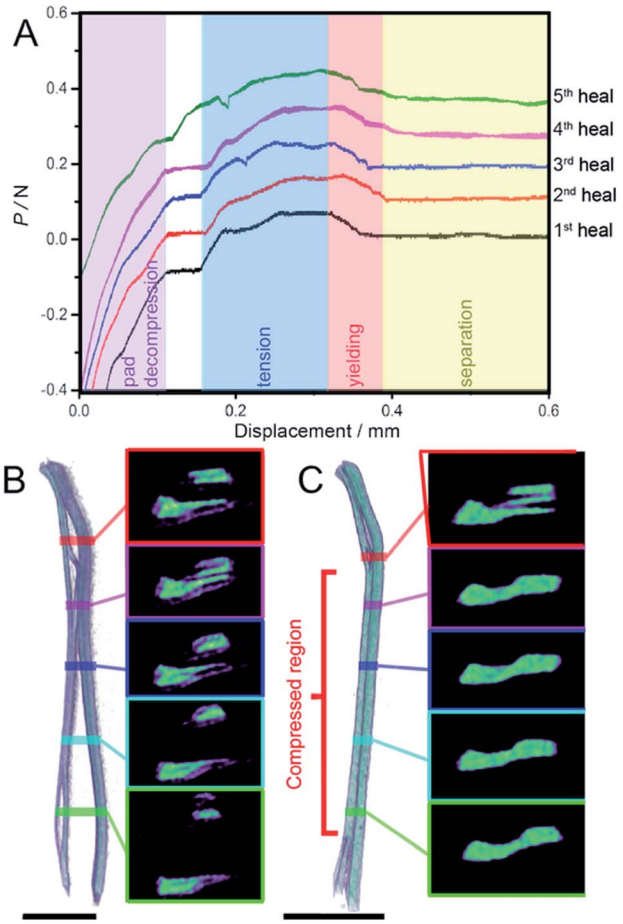

Fig. 4 Self-healing properties of the crystal of **3**. (A) Load (P)-displacement profile of a healed crystal for the first five consecutive healing attempts. A vertical offset to the loads has been added for clarity. (B and C) A 3D CT scan and cross-sectional images along the long axis of the crystal are shown before healing (B) and after being in contact for 24 h (C). Scale bars: (B and C) 1 mm.

bulk of the fragments was retained after healing, as shown by the strong and discrete X-ray diffraction pattern before and after healing (Fig. 3E and F). Since single crystal X-ray diffraction provides information on the bulk of the crystal, this result confirms that the interior of the sample remains crystalline.

To verify whether the healing behavior was caused by other interactions (physical adhesion, water cohesion, electrostatics, or other secondary effects) the tensile strength of the healed interface was measured soon after the two fragments were contacted. The two crystal faces were contacted and held together for 5 seconds, the tensile strength upon separation was measured (Fig. S5A†), and this procedure was repeated four times. A significant force holding the two fragments could not be detected, confirming that the increased tensile strength of the healed material is due to a slow process that requires sufficient time to occur during a prolonged contact. It is worth noting that not all crystals healed after being compressed for 24 h (Fig. S5B†) and we attributed it to poor contact or debris in between the pieces during compression.

The internal structure of separated and healed crystals of **3** was analyzed by using computerized tomography (CT), a technique that provides direct 3D imaging of the internal structure of the crystal based on the density distribution of the crystal interior.[21] A CT scan and selected cross-sections of a crystal of **3** before and after healing are shown in Fig. 4B and C, respectively (Movies S11 and S12†) where areas with different density of the material are displayed in different colors. Before healing the crystal is visibly separated, and the central portion of the two fragments appears denser than their periphery (Fig. 4B). After the central sections of the two fragments were put in contact with each other for 24 hours, the crystal appears mended, as seen by the more uniform color distribution in the cross-sections of the central part of the healed crystal where the two fragments were held in contact with each other (Fig. 4C).

The ubiquity of self-healing polymers stems from the intrinsic flexibility and diffusion of molecules and their parts in these disordered materials. In molecular crystalline solids, the molecules are typically thought to lack this mobility and are expected to be less able to reach and react with neighboring molecules. However, as described above, elastically and plastically bending crystal such as **3** must have a certain degree of mobility of the molecules in their structure to accommodate the molecular reorganization required for elastic and plastic bending. Indeed, the understanding of reactivity on crystal surfaces has been recently greatly advanced, and it is now accepted that mass transfer at surfaces of molecular crystals can be significant and far more than what is expected within the bulk.[21,34,35] To investigate how the surface of **3** changes over time at ambient temperature and humidity (22 °C, 37% RH) a selected area on the (100) surface was imaged by AFM over 18.5 hours (Fig. S6 and Movie S13†). Initially a step feature of the crystal was imaged and the sharp edges and steps are clearly visible (Fig. S6A†). After 7.25 hours, the step has become rounded and a series of repeated step features appeared. After 18.5 hours, the surface has flattened and several facets have formed. The direction of migration of the surface relative to the crystal faces remains unclear, because of the thermal drift and the rapid changes of the surface have removed any recognizable landmarks. Nevertheless, the results show that the crystal surface is very active and since the self-healing reaction is a surface phenomenon, a degree of mobility on the surface would aid the kinetics of the reaction.

The ester bonds in boronates are known to be dynamic in nature,[36–40] and they can be broken and reformed at room temperature. In line with this, the chemical self-healing in **3** can occur by several reactions: (a) metathesis, which is the exchange of acid and catechol between two esters (Fig. 5A) (b) transesterification (replacement of the catechol with a molecule of another free catechol) (Fig. 5A) and (c) condensation between boronic acid and catechol (Fig. 1A). The latter two processes require free reactants **1** and **2** which could be obtained on the surface of **3** by hydrolysis.

Typically, condensation of boronic acids and catechols is the proposed mechanism of self-healing in many polymers and hydrogels.[23–26] The hydrolysis of boronic esters is very well known in the dynamic covalent chemistry,[37] and not surprisingly, the surface of compound **3** was found to undergo hydrolysis when exposed to liquid or atmospheric water (Fig. S7†). Since small amounts of **1** and **2** have been observed from **3** by hydrolysis, the feasibility of condensation was tested by ball-milling pure **1** and **2** at room temperature to ensure better physical contact between the microcrystalline particles of the reactants. However, although the condensation has been reported to occur at elevated temperatures,[36] we did not observe the formation of **3** by milling and only the starting materials were found. Since the ball-milling procedures provided even harsher reaction conditions (increased shear, local heating, pressure) than simply contacting two fragments used for self-healing and condensation was not observed, we conclude that condensation of free catechol and boronic acid is not the primary mechanism of self-healing.

Transesterification between the ester and alcohol, on the other hand, requires free catechol, which can also be obtained by hydrolysis, and thus further experiments were aimed at probing whether the adhesion between the fragments was caused by hydrolysis followed by transesterification. Since the transesterification product is chemically identical to the starting material, a chemically similar yet spectroscopically distinguishable compound was used, 4-methylcatechol, to test the feasibility of transesterification on the surface. A crystal of **3** was

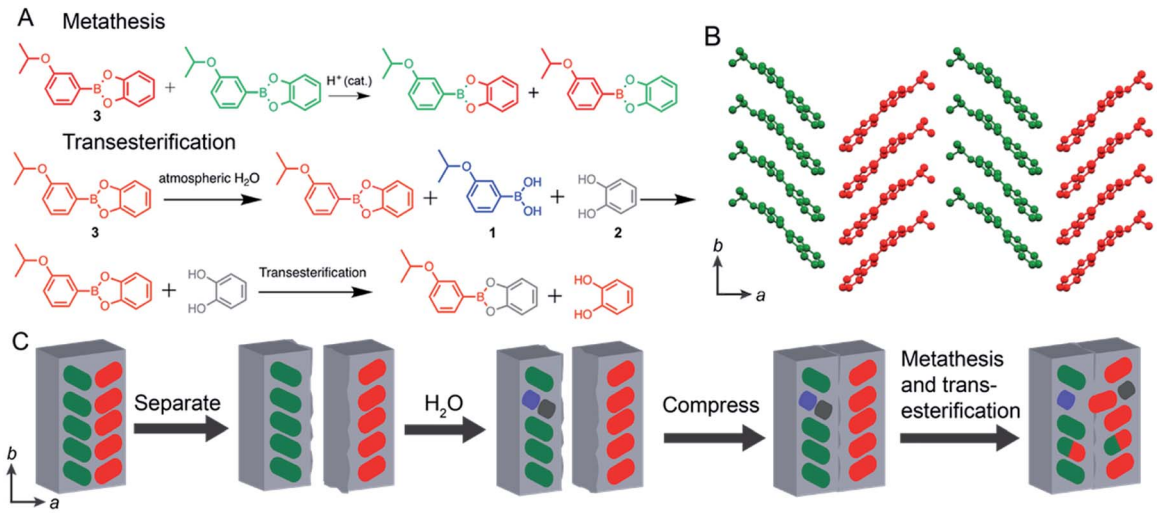

Fig. 5 Proposed mechanism of self-healing. (A) Metathesis and transesterification reactions. (B) The crystal structure of **3** showing the herringbone-type packing with the molecules from adjacent columns shown in green and red color. (C) The crystal is separated, and the fragments are mildly compressed. Metathesis occurs between the boronic ester molecules across the compressed interface. Both the green and red dots represent molecules of **3** from adjacent columns. The blue and dark grey dots represent **1** and **2**, respectively. The mixed red/green molecules represent molecules that have underwent metathesis.

placed in contact with 4-methylcatechol (0.5 N) for 16 hours and the surface of **3** was analysed using ATR FT-IR spectroscopy. The results show that the transesterification product **4** was formed after being placed in contact with 4-methylcatechol (Fig. S8A†) and the diagnostic peaks for **4** at 1488, 1359, 1317, 1162, and 821 cm^{-1} were found on the surface of **3**. The peaks from the surface of **3** can also be seen at 1567, 1467, 1369, 1232 and 968 cm^{-1}. The transesterification reaction was also found to occur by manual grinding and uniaxial pressure using powders of **3** and 4-methylcatechol (Fig. S8A and S8B†). The data shows that transesterification reaction occurs on the surface of the crystal of **3** under the same conditions as the self-healing experiments. From this, we propose transesterification is a plausible mechanism of the observed self-healing.

Finally, direct boronic ester metathesis between two adjacent molecules of **3** may reform two new molecules of **3** across the crack to achieve healing (Fig. 5A and B). The metathesis between the dynamic covalent bonds of boronic esters is known,[39,40] and it was tested by synthesizing the phenylboronic acid 4-methylcatechol ester **5**. The catechol and boronic acid components of **5** are different from those of **3**, and if ester metathesis occurred the mixed products could be detected and quantified. Representative reactions in solution and on powderized samples were performed using a ball mill to test the feasibility of this mechanism (Fig. S9†). In a solution of dimethyl sulfoxide-d_6 equimolar ratios of compounds **3** and **5** were found to metathesize readily and form boronic esters **4** and **6** (Fig. S9A†). Equimolar ratios of **3** and **5** were also ball-milled and formation of the two new boronic esters **4** and **6** was observed by the appearance of the doublets at 7.19 and 8.11 ppm corresponding to the metathesis products **4** and **6**, respectively, proving the reaction occurs in the solid state (Fig. S9B†). To remove the possible effect of shear strain on the outcome of the metathesis in the above ball-milling reactions, the effect of static pressure was also investigated using a hydraulic press. Manually ground equimolar mixtures of **3** and **5** with 0.1 mol% of phenylboronic acid were exposed to 555 MPa of pressure for varying durations (Fig. S10A†). The percent composition of esters **4** and **6** was found to be 9, 13, 12, 12 and 13% for **4** and 6, 9, 13, 13 and 13% for **6** after 0.16, 1.5, 3.6, 6 and 24 hours of compression. The same experiment was also performed with varying loads (55.5, 221, 388, and 555 MPa) with a constant duration (4 h) and formation of **4** and **6** was observed with increasing force (Fig. S10B†).

Since the pressures used here are higher than those applied to keep the two fragments in contact during the tensile measurements (~1 MPa), this result generally reflects the propensity of the ester molecules to react across the interparticle interface. Altogether, the evidence of significant exchange between boronic esters *via* metathesis upon manual grinding, ball-milling and even uniaxial pressure in the solid state supports the proposed mechanism of self-healing by metathesis.

There is a chance a portion of the restoration could stem from physical adhesion from non-covalent interactions, such as the van der Waals forces between adjacent layers. However, these interactions typically occur on the seconds scale,[41] and thus they are kinetically much faster than solid-state covalent reactions across static interfaces, which require hours for diffusion.[21] If the non-covalent interactions and physical adhesion contributed to a significant portion of the healing, we would have expected to have measured it during the 5 second compression tests and none were observed (Fig. S5A†). To further test this possibility, we developed a custom AFM experiment in which we adhered an approximately 190 × 160 μm crystal of **3** to a tipless AFM cantilever and performed surface adhesion force measurements between a macroscopic crystal of **3** and the cantilever to which the crystal was mounted (Fig. 6). The adhesion force between the crystal-mounted cantilever and the macroscopic crystal was found to be −56.42 ± 1.52 nN over 15 measurements (Table S3†). As a control, the adhesion force between the crystal attached cantilever and a sapphire surface was measured and found to be −39.77 ± 2.39 nN over three measurements (Fig. S11 and Table S4†). The results show that the adhesive properties of crystals of **3** to itself are comparable to its adhesion to sapphire, a known non-adhesive material.[42] This result eliminates the possibility of the self-healing being due to a simple physical adhesion between two crystals of **3**.

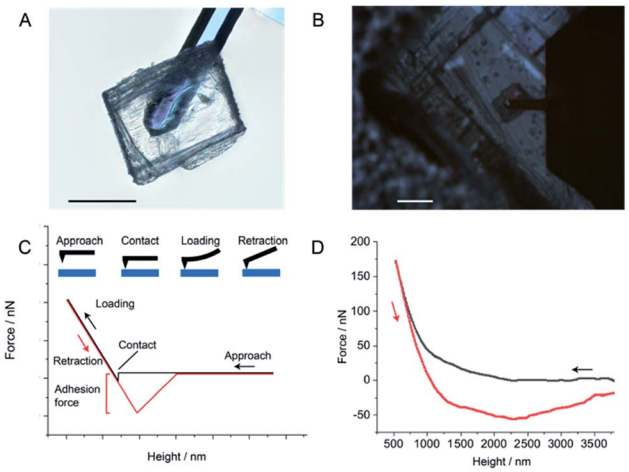

Fig. 6 AFM adhesion force experiments using a cantilever mounted with a crystal of **3**. (A) An optical image of a crystal of **3** mounted on a tipless AFM cantilever. (B) An optical image of the crystal-mounted cantilever above the surface of a macroscopic crystal of **3**. (C) A representative schematic of the adhesion force experiments. (D) The adhesion force measured between the crystal-mounted cantilever and the surface of a crystal of **3**. Scale bars: (A) 100 μm; (B) 200 μm.

Conclusions

Through our investigation of the mechanism of self-healing it is clear that both transesterification and metathesis occur in the solid state and both probably occur concurrently during the self-healing experiments. The two processes are both initiated by the same stimulus, mechanical force, and it is not possible to deconvolute the individual contributions of two mechanisms towards healing. In fact, both processes occurring simultaneously may be the reason the crystals can heal to such high

efficiencies. From this, we believe that both transesterification and metathesis are responsible for the self-healing effect (Fig. 5). If a portion of the restoration stemmed from physical adhesion by non-covalent interactions, we would have expected to have measured it during AFM adhesion experiments (Fig. 6, Tables S3 and S4†). On the other hand, the formation of the transesterification and metathesis products provides firm evidence that the bond shuffling between the boronic esters and catechol occurs in the solid state and appears to be the most likely reason for the self-healing. The reformation of the bonds between the layers is related to intrinsic self-healing capability. Within a broader context, we anticipate that self-healing by dynamic covalent chemistry is a more common phenomenon occurring in molecular crystals that can be deformed plastically, and can be explored within the realm of materials for electronics, robotics and pharmaceutical applications.

Conflicts of interest

The authors declare no conflict of interest.

Acknowledgements

This research work was sponsored in part by New York University Abu Dhabi and was partially carried out using Core Technology Platform resources at New York University Abu Dhabi. We thank Dr Liang Li for help with face indexing and Dr Stefan Schramm for help with data and image processing.

Notes and references

1 S. R. White, N. R. Sottos, P. H. Geubelle, J. S. Moore, M. R. Kessler, S. R. Sriram, E. N. Brown and S. Viswanathan, *Nature*, 2001, **409**, 794–797.
2 J. Cui, D. Daniel, A. Grinthal, K. Lin and J. Aizenberg, *Nat. Mater.*, 2015, **14**, 790–795.
3 S. H. Cho, S. R. White and P. V. Braun, *Adv. Mater.*, 2009, **21**, 645–649.
4 N. Holten-Andersen, M. J. Harrington, H. Birkedal, B. P. Lee, P. B. Messersmith, K. Y. C. Lee and J. H. Waite, *Proc. Natl. Acad. Sci. U. S. A.*, 2011, **108**, 2651–2655.
5 M. Burnworth, L. Tang, J. R. Kumpfer, A. J. Duncan, F. L. Beyer, G. L. Fiore, S. J. Rowan and C. Weder, *Nature*, 2011, **472**, 334–337.
6 A. Phadke, C. Zhang, B. Arman, C.-C. Hsu, R. A. Mashelkar, A. K. Lele, M. J. Tauber, G. Arya and S. Varghese, *Proc. Natl. Acad. Sci. U. S. A.*, 2012, **109**, 4383–4388.
7 J. Hentschel, A. M. Kushner, J. Ziller and Z. Guan, *Angew. Chem., Int. Ed.*, 2012, **51**, 10561–10565.
8 J. Canadell, H. Goossens and B. Klumperman, *Macromolecules*, 2011, **44**, 2536–2541.
9 X. Chen, M. A. Dam, K. Ono, A. Mal, H. Shen, S. R. Nutt, K. Sheran and F. A. Wudl, *Science*, 2002, **295**, 1698–1702.
10 P. A. Pratama, M. Sharifi, A. M. Peterson and G. R. Palmese, *ACS Appl. Mater. Interfaces*, 2013, **5**, 12425–12431.
11 Y. Yang and M. W. Urban, *Chem. Soc. Rev.*, 2013, **42**, 7446–7467.
12 E. B. Murphy and F. Wudl, *Prog. Polym. Sci.*, 2010, **35**, 223–251.
13 R. P. Wool, *Soft Matter*, 2008, **4**, 400–418.
14 D. L. Taylor and M. In Het Panhuis, *Adv. Mater.*, 2016, **28**, 9060–9093.
15 P. Naumov, S. Chizhik, M. K. Panda, N. K. Nath and E. Boldyreva, *Chem. Rev.*, 2015, **115**, 12440–12490.
16 G. Liu, J. Liu, X. Ye, L. Nie, P. Gu, X. Tao and Q. Zhang, *Angew. Chem., Int. Ed.*, 2017, **56**, 198–202.
17 L. Zhang, J. B. Bailey, R. H. Subramanian, A. Groisman and F. A. Tezcan, *Nature*, 2018, **557**, 86–91.
18 L. Zhu, R. O. Al-Kaysi and C. J. Bardeen, *Angew. Chem., Int. Ed. Engl.*, 2016, **55**, 7073–7076.
19 M. Jin, T. Sumitani, H. Sato, T. Seki and H. Ito, *J. Am. Chem. Soc.*, 2018, **140**, 2875–2879.
20 C. R. R. Adolf, S. Ferlay, N. Kyritsakas and M. W. Hosseini, *J. Am. Chem. Soc.*, 2015, **137**, 15390–15393.
21 P. Commins, H. Hara and P. Naumov, *Angew. Chem., Int. Ed.*, 2016, **55**, 13028–13032.
22 Y. Jin, C. Yu, R. J. Denman and W. Zhang, *Chem. Soc. Rev.*, 2013, **42**, 6634–6654.
23 O. R. Cromwell, J. Chung and Z. Guan, *J. Am. Chem. Soc.*, 2015, **137**, 6492–6495.
24 L. He, D. E. Fullenkamp, J. G. Rivera and P. B. Messersmith, *Chem. Commun.*, 2011, **47**, 7497–7499.
25 B. K. Ahn, D. W. Lee, J. N. Israelachvili and J. H. Waite, *Nat. Mater.*, 2014, **13**, 867–872.
26 W. L. A. Brooks and B. S. Sumerlin, *Chem. Rev.*, 2016, **116**, 1375–1397.
27 A. Worthy, A. Grosjean, M. C. Pfrunder, Y. Xu, C. Yan, G. Edwards, J. K. Clegg and J. C. McMurtrie, *Nat. Chem.*, 2017, **10**, 65–69.
28 G. R. Krishna, R. Devarapalli, G. Lal and C. M. Reddy, *J. Am. Chem. Soc.*, 2016, **138**, 13561–13567.
29 A. D. Herrera-España, G. Campillo-Alvarado, P. Román-Bravo, D. Herrera-Ruiz, H. Höpfl and H. Morales-Rojas, *Cryst. Growth Des.*, 2015, **15**, 1572–1576.
30 A. S. Luyt, J. A. Molefi and H. Krump, *Polym. Degrad. Stab.*, 2006, **91**, 1629–1636.
31 W. van der Zee and J. L. Urai, *J. Struct. Geol.*, 2005, **27**, 2281–2300.
32 M. K. Panda, S. Ghosh, N. Yasuda, T. Moriwaki, G. D. Mukherjee, C. M. Reddy and P. Naumov, *Nat. Chem.*, 2015, **7**, 65–72.
33 J. Ling, M. Z. Rong and M. Q. Zhang, *Polymer*, 2012, **53**, 2691–2698.
34 G. Kaupp and M. R. Naimi-Jamal, *CrystEngComm*, 2005, **7**, 402–410.
35 S. Varughese, M. S. R. N. Kiran, U. Ramamurty and G. R. Desiraju, *Angew. Chem., Int. Ed. Engl.*, 2013, **52**, 2701–2712.
36 G. Kaupp, M. R. Naimi-Jamal and V. Stepanenko, *Chem.–Eur. J.*, 2003, **9**, 4156–4161.
37 S. D. Bull, M. G. Davidson, J. M. H. van den Elsen, J. S. Fossey, A. T. Jenkins, Y.-B. Jiang, Y. Kubo, F. Marken, K. Sakurai, J. Zhao and T. D. James, *Acc. Chem. Res.*, 2013, **46**, 312–326.

38 R. Nishiyabu, Y. Kubo, T. D. James and J. S. Fossey, *Chem. Commun.*, 2011, **47**, 1124–1150.
39 C. D. Roy and H. C. Brown, *J. Organomet. Chem.*, 2007, **692**, 784–790.
40 M. Röttger, T. Domenech, R. van der Weegen, A. Breuillac, R. Nicolaÿ and L. Leibler, *Science*, 2017, **356**, 62–65.
41 K. Autumn, Y. A. Liang, S. T. Hsieh, W. Zesch, W. P. Chan, T. W. Kenny, R. Fearing and R. J. Full, *Nature*, 2000, **405**, 681–685.
42 H. Zhou, Q. Xu, S. Li, Y. Zheng, X. Wu, C. Gu, Y. Chen and J. Zhong, *RSC Adv.*, 2015, **5**, 91633–91639.